Relativistic electromagnetic ion cyclotron instabilities

K. R. Chen,* R. D. Huang, J. C. Wang, and Y. Y. Chen
Department of Physics and Institute of Electro-Optical Science and Engineering, National Cheng Kung University, Tainan 701, Taiwan, Republic of China
(Received 26 June 2004; published 24 March 2005)

The relativistic instabilities of electromagnetic ion cyclotron waves driven by MeV ions are analytically and numerically studied. As caused by wave magnetic field and in sharp contrast to the electrostatic case, interesting characteristics such as Alfvénic behavior and instability transition are discovered and illuminated in detail. The instabilities are reactive and are raised from the coupling of slow ions' first-order resonance and fast ions' second-order resonance, that is an essential extra mechanism due to relativistic effect. Because of the wave magnetic field, the nonresonant plasma dielectric is usually negative and large, that affects the instability conditions and scaling laws. A negative harmonic cyclotron frequency mismatch between the fast and slow ions is required for driving a cubic (and a coupled quadratic) instability; the cubic (square) root scaling of the peak growth rate makes the relativistic effect more important than classical mechanism, especially for low fast ion density and Lorentz factor being close to unity. For the cubic instability, there is a threshold (ceiling) on the slow ion temperature and density (the external magnetic field and the fast ion energy); the Alfvén velocity is required to be low. This Alfvénic behavior is interesting in physics and important for its applications. The case of fast protons in thermal deuterons is numerically studied and compared with the analytical results. When the slow ion temperature or density (the external magnetic field or the fast ion energy) is increased (reduced) to about twice (half) the threshold (ceiling), the same growth rate peak transits from the cubic instability to the coupled quadratic instability and a different cubic instability branch appears. The instability transition is an interesting new phenomenon for instability.

DOI: 10.1103/PhysRevE.71.036410 PACS number(s): 52.55.Pi, 52.27.Ny, 52.35.Hr, 52.35.Qz

I. INTRODUCTION

Electromagnetic cyclotron instability is an important mechanism in magnetized plasmas and is an active research area in plasma physics and wave dynamics [1–4] with applications for coherent radiation [1,2,5], heating [6,7], current drive [8–10], and diagnostic [11] in laboratory [12,13], industrial [14], space [15,16], and astrophysical [17] plasmas. While the relativistic effect has been well known for five decades to be essential for electromagnetic electron cyclotron instability [1,2,18–22], the importance of relativity for ion cyclotron instability is discovered for only one decade [23–30] because the Lorentz factor of ions is very close to unity in typical plasmas due to the large ion mass. Indeed, the fact that the relativistic effect with a very small Lorentz factor -1 can play an essential role to affect fast ion dynamics significantly [25,27,29,30] is very interesting in fundamental physics. Furthermore, the polarization of the waves studied so far is electrostatic [23–30]; that is, the wave vector is parallel to the electric field and there is no wave magnetic field.

The dynamics and stability of fast ions produced in fusion reactions are critical for maintaining the burning of plasmas in fusion reactors [31–33]. The fast ion cyclotron emissions measured in reactors [34–38] provide a means to understand the fast ions' dynamics. Electromagnetic ion cyclotron instability [39,40], relativistic electrostatic ion cyclotron instability [23,24,28], and magnetoacoustic instability [41,42] have been proposed to explain the emissions. The electromagnetic ion cyclotron instability is excited by the fast ions due to inversed Landau damping [39], without considering relativity. In fusion reactors, the fast ion density is much lower than that of the slow ions. Because the growth rate is proportional to the fast ion density, the electromagnetic ion cyclotron instability is weak [39]. Also, since the inversed Landau damping requires an exact resonance, the fast ions may only remain in resonance within a small part of their circulation trajectory such that the effective fast ion density can be a few orders smaller [40]. On the other hand, the relativistic electrostatic ion cyclotron instability is driven by the fast ions through the coupling of slow ions' first-order resonance and fast ions' second-order resonance in the susceptibility at the same direction of the wave vector and the electric field. When the harmonic cyclotron frequency mismatch of fast and slow ions is negative (e.g., fast protons in thermal deuterons), these two cyclotron streams in gyrophase are coupled to excite a cubic instability and a coupled quadratic instability. When it is positive (e.g., fast alphas in thermal deuterons), a decoupled quadratic instability can be driven only at high harmonics where the slow ions are cold.

In this paper, the relativistic electromagnetic ion cyclotron instability and its physics are studied. The dispersion relation for electromagnetic wave propagating across an external magnetic field is derived from relativistic kinetic theory and, then, is analyzed for the wave frequency near the harmonic ion cyclotron frequencies of the plasmas consisting of fast ions, Maxwellian slow ions, and electrons. Both a cubic instability and a quadratic instability raised from the coupling offast and slow ion cyclotron harmonics are found when the frequency mismatch is negative; due to the wave magnetic

*Electronic address: chenkr@mail.ncku.edu.tw

 ©2005 The American Physical Society

field, the decoupled quadratic instability cannot be driven even at high harmonics as in contrast to the electrostatic case. The peak growth rate is scaled as the cubic or square root of the fast ion density. This makes the relativistic effect more important than the classical inversed Landau damping for driving electromagnetic ion cyclotron instability. Also due to the wave magnetic field, the characteristics and conditions of the relativistic electromagnetic instabilities are quite different with the electrostatic instability. For example, the Alfvénic behavior is revealed, that is important for applications. By moderately changing plasma parameters, we observe an interesting physical phenomenon; that is, the same growth rate peak can transit from the cubic instability to the quadratic instability and then a new cubic branch appears.

The susceptibility and dispersion relation for the electromagnetic wave perpendicular to the external magnetic field will be derived from relativistic kinetic theory in the next section. Section III is the instability analysis of electromagnetic ion cyclotron waves in resonance with one fast ion species and maybe also with a Maxwellian slow ion species. Section IV is for the numerical studies of fast protons in thermal deuterons, based on typical plasma parameters. The discussions and the summary are given in Sec. V.

II. DISPERSION RELATION FROM RELATIVISTIC KINETIC THEORY

Consider a uniform plasma under an external magnetic field in the z direction (i.e., $\vec{B}_0=B_0\hat{z}$) and an electromagnetic wave with its electric field polarized in the y direction propagating along the x direction with its wave vector $\vec{k}=k\hat{x}$. The dispersion relation for this electromagnetic wave in the plasma is given as

$$1-\frac{k^2c^2}{\omega^2}+\chi=0, \tag{1}$$

where c is the speed of light, ω is the wave frequency, χ is the susceptibility constant in the y direction. Derived from the Vlasov equation and Maxwell equations, the susceptibility is [13]

$$\chi=\sum_{species}\sum_{n=-\infty}^{\infty}\int_0^{\infty}2\pi P_\perp dP_\perp\int_{-\infty}^{\infty}dP_z\frac{\omega_p^2}{\omega}\frac{[J_n'(k\rho)]^2P_\perp\frac{\partial f_0}{\partial P_\perp}}{\omega-n\omega_c}, \tag{2}$$

where the susceptibility constant includes all species of the plasma, n is the harmonic number, $P_\perp(P_z)$ is the perpendicular (parallel) momentum, $\omega_p=(4\pi n_0q^2/\gamma m)^{1/2}$ is the plasma frequency, n_0 is the plasma density, q is the charge, γ is the Lorentz factor, m is the rest mass, $\omega_c=\Omega_c/\gamma$ is the cyclotron frequency, $\Omega_c=qB_0/mc$ is the nonrelativistic cyclotron frequency, $J_n'(k\rho)$ is the derivative of Bessel function of first kind of order n with the parameter $k\rho$, $\rho=v_\perp/\omega_c$ is the gyroradius, $v_\perp$ is the perpendicular gyrovelocity, and f_0 is the distribution function.

Equation (2) is integrated by part and substituted into Eq. (1) to yield the relativistic dispersion relation for the electromagnetic waves as

$$0=1-\frac{k^2c^2}{\omega^2}-\sum_{species}\sum_{n=-\infty}^{\infty}\int_0^{\infty}2\pi P_\perp dP_\perp\int_{-\infty}^{\infty}dP_zf_0\frac{\omega_p^2}{\omega^2}\times\left\{\frac{\omega}{2n(\omega-n\omega_c)}(n^2-k^2\rho^2)[J_{n-1}^2(k\rho)-J_{n+1}^2(k\rho)]-\left(\frac{\omega^2}{(\omega-n\omega_c)^2}\frac{\omega_c^2}{k^2c^2}k^2\rho^2[J_n'(k\rho)]^2\right)_{\text{relat}}\right\}. \tag{3}$$

The term within parentheses with subscript "relat" is due to the inclusion of relativity. Mathematically, this term comes from the derivative of the cyclotron frequency in the resonance condition because of $\partial\gamma/\partial P_\perp=P_\perp/(\gamma m^2c^2)$ [1,2,23,28]. Physically, the inclusion of the relativistic Lorentz factor in the cyclotron frequency provides a mechanism for the energy exchange between the plasma and the wave through the relativistic cyclotron resonance [1,2,23,28].

If the plasma consists of fast ions as well as Maxwellian slow ions and electrons, the dispersion relation for the electromagnetic wave with a frequency much lower than the electron cyclotron frequency becomes

$$0=1-\frac{k^2c^2}{\omega^2}+\frac{\omega_{pe}^2}{\omega_{ce}^2}-\sum_{slow}\sum_{s=-\infty}^{\infty}\left\{\frac{\omega_{ps}^2}{\omega(\omega-s\omega_{cs})}h_s(\lambda)-\left(\frac{\omega_{ps}^2}{(\omega-s\Omega_{cs})^2}\frac{T}{m_sc^2}h_s(\lambda)\right)_{\text{relat}}\right\}-\sum_{fast}\sum_{\ell=-\infty}^{\infty}\left\{\frac{\omega_{pf}^2}{2\ell\omega(\omega-\ell\omega_{cf})}[\ell^2\langle J_{\ell-1}^2\rangle-\ell^2\langle J_{\ell+1}^2\rangle-\langle k^2\rho^2J_{\ell-1}^2\rangle+\langle k^2\rho^2J_{\ell+1}^2\rangle]-\left(\frac{\omega_{pf}^2\omega_{cf}^2}{2k^2c^2(\omega-\ell\omega_{cf})^2}\times[\langle k^2\rho^2J_{\ell-1}^2\rangle+\langle k^2\rho^2J_{\ell+1}^2\rangle-2\ell^2\langle J_\ell^2\rangle]\right)_{\text{relat}}\right\}, \tag{4}$$

where

$$h_s(\lambda)=\left[\frac{s^2I_s(\lambda)}{\lambda}+2\lambda I_s(\lambda)-2\lambda I_s'(\lambda)\right]e^{-\lambda} \tag{5}$$

$$\cong\frac{s^2\lambda^{|s|-1}}{2^{|s|}|s|!}\quad\text{if }\lambda\ll1, \tag{6}$$

$h_{-s}=h_s$; s (ℓ) is the harmonic number of the slow (fast) ions; the subscripts e, s, and f are for electron, slow, and fast ions, respectively; T is the slow ion temperature assumed to be low so that $\gamma_s\simeq1$; $\lambda=(k^2T/m_s\Omega_s^2)=k^2\rho_s^2$; ρ_s is the Larmor radius of the thermal slow ions; I_s is the modified Bessel function of first kind of order s; I_s' is the derivative of I_s; $\langle(\cdots)\rangle=\int d^3Pf_0(\cdots)$ is averaged over a momentum distribution; for an isotropic distribution $f_0=\delta(\vec{P}-P_0\hat{r})/4\pi P_0^2$ (e.g., fast ions produced by fusion reaction),

$$\langle J_\ell^2\rangle=\frac{1}{2}\int_0^{\pi}\sin\theta d\theta J_\ell^2(k\rho_0\sin\theta), \tag{7}$$

$$\langle k^2\rho^2 J_\ell^2\rangle = \frac{1}{2}\int_0^\pi \sin^3\theta d\theta k^2\rho_0^2 J_\ell^2(k\rho_0\sin\theta); \tag{8}$$

for a beam distribution $f_0=\delta(P_\perp-P_{\perp 0})\delta(P_z-P_{z0})/2\pi P_{\perp 0}$ (e.g., neutron beam injection),

$$\langle J_\ell^2\rangle = J_\ell^2(k\rho_{\perp 0}), \tag{9}$$

$$\langle k^2\rho^2 J_\ell^2\rangle = k^2\rho_{\perp 0}^2 J_\ell^2(k\rho_{\perp 0}); \tag{10}$$

the fast ion Larmor radius $\rho_{\perp 0}=P_{\perp 0}/m_f\Omega_{cf}=v_{\perp 0}/\omega_{cf}$; and $\rho_0=P_0/m_f\Omega_{cf}=v_0/\omega_{cf}$.

III. CYCLOTRON INSTABILITY ANALYSIS FOR ONE FAST ION SPECIES

Without loss of generality, we will consider one fast ion species with its ℓth harmonic cyclotron frequency in resonance with the wave frequency and maybe also with the sth harmonic cyclotron frequency of one of the slow ion species (i.e., $\ell\omega_{cf}\cong\omega\cong s\omega_{cs}$). The relativistic term of the slow ion in Eq. (4) can be neglected if the slow ion temperature is low. Thus the dispersion relation for the electromagnetic ion cyclotron waves in the plasma can be written as

$$0 = A + \frac{D}{(\omega-\ell\omega_{cf})+\Delta} + \frac{B}{\omega-\ell\omega_{cf}} + \frac{C}{(\omega-\ell\omega_{cf})^2}, \tag{11}$$

where

$$A = 1 - \frac{k^2c^2}{\omega^2} + \frac{\omega_{pe}^2}{\omega_{ce}^2} - \sum_{slow,s\neq 1}\frac{2\omega_{ps}^2}{\ell^2\omega_{cf}^2-\Omega_{cs}^2}h_1, \tag{12}$$

$$B = -\frac{\omega_{pf}^2}{2\omega_{cf}}\left[\langle J_{\ell-1}^2\rangle - \langle J_{\ell+1}^2\rangle - \frac{1}{\ell^2}\langle k^2\rho^2 J_{\ell-1}^2\rangle + \frac{1}{\ell^2}\langle k^2\rho^2 J_{\ell+1}^2\rangle\right], \tag{13}$$

$$C = \frac{\omega_{pf}^2\omega_{cf}^2}{2k^2c^2}[\langle k^2\rho^2 J_{\ell-1}^2\rangle + \langle k^2\rho^2 J_{\ell+1}^2\rangle - 2\ell^2\langle J_\ell^2\rangle], \tag{14}$$

$$D = -\frac{\omega_{ps}^2}{\ell\omega_{cf}}h_s(\lambda), \tag{15}$$

$$\Delta = \ell\omega_{cf} - s\omega_{cs} \cong \ell\omega_{cf}\left(1-\frac{s\Omega_{cs}}{\ell\Omega_{cf}}\gamma\right) \ll \ell\omega_{cf}. \tag{16}$$

The coefficient A is the nonresonant plasma dielectric that represents the plasma inertia. The summation in A sums over all slow ion species whose first harmonic is not in resonance. The coefficient B is the first-order resonance of the fast ion. The instability driving is from the second-order resonance of the fast ion due to the relativistic effect, that is with a coefficient C. The slow ion's resonance is first-order with a coefficient D, that represents the resonant slow ion inertia. We note that $D=0$ if no slow ion harmonic number s can satisfy the resonance condition. The dispersion relation in Eq. (11) is written in a format being the same as that of the relativistic electrostatic ion cyclotron waves [23,28]. But, there are significant differences important for determining the instability characteristics. For the electromagnetic wave, there is an extra dielectric $-k^2c^2/\omega^2$ contributed by the wave magnetic field in the nonresonant dielectric A. This extra dielectric is a negative number with its absolute value much larger than unity due to low wave phase velocity and thus makes the plasma inertia usually negative and large, that is a negative effect for driving instabilities. The coefficient C of the electromagnetic case is proportional to the square of the derivative of Bessel function in contrast to the square of Bessel function in the electrostatic case, while the coefficient B in both cases are related to the derivative of Bessel function.

For instability analysis, the dispersion relation can be rewritten as a cubic algebraic equation of the difference between the wave frequency and the harmonic fast ion cyclotron frequency; that is,

$$0 = (\omega-\ell\omega_{cf})^3 + P(\omega-\ell\omega_{cf})^2 + Q(\omega-\ell\omega_{cf}) + R, \tag{17}$$

$$P = \Delta + \frac{B+D}{A}, \tag{18}$$

$$Q = \frac{B\Delta + C}{A}, \tag{19}$$

$$R = \frac{C\Delta}{A}. \tag{20}$$

The characteristics of the instability is mainly determined by P (i.e., $A\Delta+D$, if the fast ion density is much lower than the slow ion density), that indicates the competition between the harmonic cyclotron frequency mismatch and the resonant slowion dielectric normalized by the nonresonant plasma dielectric. The parameter R is the driving parameter defined as the driving dielectric coefficient of the fast ion second-order resonance normalized by the nonresonant plasma dielectric multiplying the frequency mismatch. We consider that the phase velocity of the wave is much slower than the speed of light, the Lorentz factor of the fast ions is close to unity, and the slow ion gyroradius is small (i.e., $\lambda\ll 1$). Thus

$$A \simeq -\frac{k^2c^2}{\ell^2\omega_{cf}^2} - \sum_{slow,s\neq 1} a_s\frac{\omega_{ps}^2}{\ell^2\omega_{cf}^2}, \tag{21}$$

$$\Delta \simeq -\ell\omega_{cf}\delta\gamma(1+a_m), \tag{22}$$

$$D \simeq -\frac{1}{\ell\omega_{cf}}\left(\frac{s^2}{2^s s!}\omega_{ps}^2\lambda^{s-1}\right), \tag{23}$$

$$a_s = \left(1-\frac{\Omega_{cs}^2}{\ell^2\omega_{cf}^2}\right)^{-1}, \tag{24}$$

$$a_m = \frac{\delta m_s - \delta m_f}{\delta\gamma}, \tag{25}$$

where $\delta\gamma=\gamma-1$, $\delta m=1-m/Nm_p$ is defined as the normalized mass deficit per nucleon of the ions, N is the nucleon

number of the ions, and m_p is the proton rest mass.

A. Cubic instability

The first case to be studied is $A\Delta+D\simeq 0$ or $P\simeq 0$ (i.e., $|P|\ll|\omega-\ell\omega_{cf}|$). Since both A and D are negative, this requires the harmonic cyclotron frequency mismatch between the fast ions and the slow ions being negative (i.e., $\Delta<0$). A cubic instability may be driven due to the coupling of the second-order fast ion resonance and the first-order slow ion resonance. Substituting Eqs. (21)–(23) into this equality yields

$$0 \simeq A\Delta + D \tag{26}$$

$$= \frac{1+a_m}{\ell\omega_{cf}}\left[\frac{k^2\rho_0^2\omega_{cf}^2}{2} + \delta\gamma\sum_{slow,s\neq 1} a_s\omega_{ps}^2 - \frac{s^2}{2^s s!(1+a_m)}\omega_{ps}^2\lambda^{s-1}\right]. \tag{27}$$

If the first slow ion cyclotron harmonic is in resonance (i.e., $s=1$), this indicates

$$k\rho_o \simeq \frac{\omega_{ps}}{\omega_{cf}}\frac{1}{\sqrt{1+a_m}}. \tag{28}$$

When the resonant slow ion cyclotron harmonic number is 2 (i.e., $s=2$), this equality occurs at

$$k\rho_0 \simeq \left[\frac{2\delta\gamma\Sigma_{slow,s\neq 1}a_s\omega_{ps}^2}{\frac{1}{1+a_m}\frac{\rho_s^2}{\rho_f^2}\omega_{ps}^2-\omega_{cf}^2}\right]^{1/2}, \tag{29}$$

if the condition

$$\frac{v_{\perp s}^2}{v_{\perp 0}^2} > (1+a_m)\frac{c_A{}^2}{c^2}, \tag{30}$$

that is,

$$\frac{T}{E_f} > 2(1+a_m)\frac{m_s}{m_f}\frac{\Omega_s^2}{\omega_{ps}^2} = \frac{1+a_m}{2\pi m_f c^2}\frac{B^2}{n_s}, \tag{31}$$

can be satisfied because the denominator of Eq. (29) has to be positive; where $v_{\perp s}=(T/m_s)^{1/2}$ is the perpendicular slow ion thermal velocity, $c_A=c\Omega_{cs}/\omega_{ps}=B/(4\pi n_s m_s)^{1/2}$ is the Alfvén velocity, E_f is the fast ion energy, and n_s is the slow ion density. Alfvén velocity is required to be low. There is a threshold (ceiling) on the slow ion temperature and density (the external magnetic field and the fast ion energy). This Alfvénic condition mainly comes from the k^2c^2/ω^2 dielectric contributed by the wave magnetic field and does not exist in the electrostatic instabilities. If the resonant slow ion cyclotron harmonic number is larger than two (i.e., $s>2$), Eq. (27) cannot be satisfied for typical plasma parameters because of low slow ion temperature as compared with fast ion energy (i.e., $\lambda\ll 1$).

Define

$$a = Q - P^2/3, \tag{32}$$

$$b = R - PQ/3 + 2P^3/27. \tag{33}$$

A pair of complex conjugate roots exist for the cubic dispersion relation in Eq. (17) if [43]

$$\frac{b^2}{4}+\frac{a^3}{27} > 0. \tag{34}$$

Since a is usually negative, the condition becomes $b^2/4 > |a^3/27|$. This condition can be satisfied if Q is also small; that is, $B\Delta+C\approx 0$. Thus, at $P\simeq 0$ and $Q\simeq 0$, the real and imaginary parts of the wave frequency at the maximum growth rate, respectively, are [43]

$$\omega_r \simeq \ell\omega_{cf} + \frac{1}{2}\sqrt[3]{\frac{C\Delta}{A}} \tag{35}$$

$$\simeq \ell\omega_{cf}\left\{1+\frac{1}{2}\left[\frac{\omega_{pf}^2\omega_{cf}^2}{k^4c^4}\delta\gamma(1+a_m)\langle k^2\rho^2[J_\ell'(k\rho)]^2\rangle\right]^{1/3}\right\}, \tag{36}$$

$$\omega_{i,max} \simeq \frac{\sqrt{3}}{2}\sqrt[3]{R}\left(1+\frac{a}{3b^{2/3}}\right) \tag{37}$$

$$\simeq \frac{\sqrt{3}}{2}\sqrt[3]{\frac{C\Delta}{A}} \tag{38}$$

$$\simeq \frac{\sqrt{3}}{2}\ell\omega_{cf}\left[\frac{\omega_{pf}^2\omega_{cf}^2}{k^4c^4}\delta\gamma(1+a_m)\langle k^2\rho^2[J_\ell'(k\rho)]^2\rangle\right]^{1/3}. \tag{39}$$

The wave frequency is slightly larger than the harmonic cyclotron frequency of fast ions and smaller than that of slow ions. Because the cubic correction term $a/b^{2/3}\simeq Q/R^{2/3}$ at $P\simeq 0$, a positive (negative) Q will slightly increase (decreases) the maximum growth rate and the frequency mismatch between the wave and the fast ion cyclotron harmonic. The peak growth rate is proportional to the cubic root of the frequency mismatch and thus the relativistic factor (i.e., $\gamma-1$). The value of the cubic root can be not small even the relativistic factor is very small. The peak growth rate is also proportional to the cubic root of the fast ion density, the frequency mismatch between the fast and slow ions, and the instability driving term C from the fast ions, and is inversely proportional to the nonresonant plasma dielectric A (i.e., the plasma inertia), as in the electrostatic instability. However, in contrast to that of the cubic relativistic electrostatic ion cyclotron instability [23,28], both the maximum growth rate and the frequency mismatch between the wave and the fast ion depend on the derivative of Bessel function. Furthermore, the $-k^2c^2/\omega^2$ dielectric can make the absolute value of A large and thus the growth rate smaller. Following is our explanation. This is contributed by the wave magnetic field. The energy of low-frequency electromagnetic wave is mostly in the wave magnetic field; but only electric field can change the energy of ions and its Lorentz factor, that is needed for

driving the relativistic instability. Higher k means less energy in the electric field part and thus makes the instability weaker.

B. Coupled quadratic instability

We are going to analyze the case of $|D| \gg |A\Delta|$, $|\Delta| > |\omega - \ell\omega_{cf}|$, and thus $|P| \gg |\omega - \ell\omega_{cf}|$. The wave frequency is closely resonant with the harmonic cyclotron frequency of fast ion, while the harmonic slow ion cyclotron acting as an inertia is still large enough to be involved in the resonance. These conditions indicate

$$\frac{\omega_{ps}^2}{\omega_{cf}^2}\frac{s^2\lambda^{s-1}}{2^s s!} \gg \left(\frac{k^2\rho_0^2}{2} + \delta\gamma \sum_{slow,s\neq 1} a_s \frac{\omega_{ps}^2}{\omega_{cf}^2}\right)|1+a_m|. \quad (40)$$

If the first slow ion cyclotron harmonic is in resonance (i.e., $s=1$), it becomes

$$k\rho_0 \ll \frac{1}{\sqrt{|1+a_m|}}\frac{\omega_{ps}}{\omega_{cf}}. \quad (41)$$

When the resonant slow ion cyclotron harmonic number is 2 (i.e., $s=2$), the inequality can be rewritten

$$\frac{1}{|1+a_m|}\frac{v_{\perp s}^2}{v_{\perp 0}^2}\frac{c^2}{{c_A}^2} - \frac{1}{k^2c^2}\sum_{slow,s\neq 1} a_s\omega_{ps}^2 \gg 1. \quad (42)$$

If the resonant slow ion cyclotron harmonic number is larger than 2 (i.e., $s>2$), the condition (40) can not be valid because $\lambda \ll 1$. Both conditions require higher slow ion density, weaker magnetic field, and lower fast ion energy, while the condition (42) also needs higher slow ion temperature.

When the above conditions can be satisfied, the dispersion relation, Eq. (17), becomes a quadratic equation of the wave frequency and both the contributions of fast and slow ions to the susceptibility remain coupled; that is,

$$0 = (D+B+A\Delta)(\omega-\ell\omega_{cf})^2 + (B\Delta+C)(\omega-\ell\omega_{cf}) + C\Delta. \quad (43)$$

The condition for the coupled quadratic relativistic electromagnetic ion cyclotron instability is

$$(B\Delta+C)^2 - 4(D+B+A\Delta)C\Delta < 0. \quad (44)$$

Since D is negative, B is small, and C is positive, a negative frequency mismatch between the fast and slow ions is also required.

For the coupled quadratic instability, the real and imaginary parts of the frequency of the most unstable wave are

$$\omega_r = \ell\omega_{cf} - \frac{B\Delta+C}{2(D+B+A\Delta)} \approx \ell\omega_{cf}, \quad (45)$$

$$\omega_{i,max} = \frac{\sqrt{4(D+B+A\Delta)C\Delta - (B\Delta+C)^2}}{2|D+B+A\Delta|} \quad (46)$$

$$\simeq \sqrt{\frac{C\Delta}{D+B+A\Delta}} \quad (47)$$

$$= \ell\omega_{cf}\left\{\frac{\omega_{pf}^2}{k^2c^2}\frac{\omega_{cf}}{2\ell}\delta\gamma(1+a_m)[\langle k^2\rho^2 J_{\ell-1}^2\rangle + \langle k^2\rho^2 J_{\ell+1}^2\rangle - 2\ell^2\langle J_\ell^2\rangle]\right\}^{1/2}[-(D+B+A\Delta)]^{-1/2}. \quad (48)$$

The peak growth rate is proportional to the square root of the driving coefficient C, the harmonic cyclotron frequency mismatch between the fast and slow ions, and thus the fast ion density and the relativistic factor. The coefficient A multiplied with the frequency mismatch is kept in the denominator to increase the accuracy of the analytical prediction because the magnitude of the coefficient A is large. Because both coefficients A and D as well as the frequency mismatch are negative, the denominator correction increases the growth rate; but, the correction should not be large, otherwise, the instability becomes the cubic instability.

C. Decoupled quadratic instability

The third parameter regime for possible instabilities is that the slow ion is too cold for its high harmonic cyclotron being involved in the resonance. Thus the fast ion drives the instability by its second-order resonance in a cold plasma. The conditions are $|A\Delta| \gg |D|$, $|\Delta| \gg |\omega - \ell\omega_{cf}|$, and thus $|P| \gg |\omega - \ell\omega_{cf}|$; that is,

$$\left(\frac{k^2\rho_0^2}{2} + \delta\gamma \sum_{slow,s\neq 1} a_s \frac{\omega_{ps}^2}{\omega_{cf}^2}\right)|1+a_m| \gg \frac{\omega_{ps}^2}{\omega_{cf}^2}\frac{s^2\lambda^{s-1}}{2^s s!}. \quad (49)$$

If the first slow ion cyclotron harmonic is in resonance (i.e., $s=1$), the inequality becomes

$$k\rho_0 \gg \frac{1}{\sqrt{|1+a_m|}}\frac{\omega_{ps}}{\omega_{cf}}. \quad (50)$$

When the resonant slow ion cyclotron harmonic number is 2 (i.e., $s=2$), the inequality can be written as

$$1 \gg \frac{1}{|1+a_m|}\frac{v_{\perp s}^2}{v_{\perp 0}^2}\frac{c^2}{{c_A}^2} - \frac{1}{k^2c^2}\sum_{slow,s\neq 1} a_s\omega_{ps}^2. \quad (51)$$

Both conditions require lower slow ion density, stronger magnetic field, and higher fast ion energy. The condition (51) further requires lower slow ion temperature. If the resonant slow ion cyclotron harmonic number is larger than 2 (i.e., $s>2$), the condition (49) can be easily satisfied because of $\lambda \ll 1$. If there is no any slow ion cyclotron harmonic in resonance with the wave and the fast ion harmonic, no condition is needed.

The dispersion relation, Eq. (11), becomes

$$A(\omega-\ell\omega_{cf})^2 + B(\omega-\ell\omega_{cf}) + C = 0, \quad (52)$$

that is in a quadratic form of the wave frequency resonating with a harmonic fast ion cyclotron frequency while the slow ions are not involved. The unstable condition of this decoupled quadratic instability is $B^2 - 4AC < 0$. Since C is positive, A has to be also positive as in the relativistic electrostatic ion cyclotron instability; but, in the electromagnetic case, the wave magnetic field contributes a large negative term so that

the decoupled quadratic instability cannot be driven at high fast ion cyclotron harmonics. If the cyclotron frequency of slow ions is larger than the wave frequency that is not resonant with the first cyclotron harmonic of slow ions, the coefficient A can be positive when

$$\frac{k^2c^2}{\ell^2\omega_{cf}^2} < \sum_{slow,s\neq 1} \frac{\omega_{ps}^2}{\Omega_{cs}^2 - \ell^2\omega_{cf}^2}. \tag{53}$$

The growth rate peaks at $B=0$. The real and imaginary parts of the frequency of the most unstable wave for this decoupled quadratic instability are

$$\omega_r \approx \ell\omega_{cf}, \tag{54}$$

$$\omega_{i,max} \approx \sqrt{\frac{C}{A}} \tag{55}$$

$$\approx \omega_{cf}\left\{\frac{\omega_{pf}^2}{2k^2c^2}[\langle k^2\rho^2 J_{\ell-1}^2(k\rho)\rangle + \langle k^2\rho^2 J_{\ell+1}^2(k\rho)\rangle - 2\ell^2\langle J_\ell^2(k\rho)\rangle]\right\}^{1/2} \times\left[1+\frac{\omega_{pe}^2}{\omega_{ce}^2} + \sum_{slow,s\neq 1}\frac{\omega_{ps}^2}{\Omega_{cs}^2-\ell^2\omega_{cf}^2} - \frac{k^2c^2}{\ell^2\omega_{cf}^2}\right]^{-1/2}. \tag{56}$$

When the nonresonant plasma dielectric A (i.e., the plasma inertia) is close to zero, the growth rate of the decoupled quadratic relativistic electromagnetic ion cyclotron instability can be large. The growth rate is proportional to the square root of the fast ion density.

IV. NUMERICAL STUDIES

To illuminate the characteristics of the relativistic electromagnetic ion cyclotron instabilities, we will study numerically the dispersion relation given in Eq. (4). The numerical results will be compared with those obtained from the analytical theory. Without loss of generality, cases with plasma parameters being typical in laboratory devices and the scaling laws of the instabilities will be investigated.

Both the cubic and coupled quadratic instabilities require a negative frequency mismatch. Proton has a nucleon with one positive charge and its rest mass is $1836.15m_e$. Since proton mass is defined as unity, the normalized mass deficit per nucleon of proton is zero (i.e., $\delta m_p=0$). Deuteron has two nucleons and one positive charge with its rest mass being $3670.48m_e$ so that the normalized mass deficit per nucleon of deuteron is $\delta m_d \simeq 0.000\,496$. The fast protons produced by fusion reaction of thermal deuterons are isotropically distributed in momentum space with an energy of 3.02 MeV so that its Lorentz factor is $\gamma_p \simeq 1.003\,22$. Thus the frequency mismatch for the fast 3.02-MeV protons in thermal deuterons is $\Delta = -0.003\,71\ell\omega_{cp}$, that can satisfy the instabilities' requirement. The α particle has four nucleons and two positive charges with its rest mass being $7294.30m_e$ so that the normalized mass deficit per nucleon of alpha particle is $\delta m_\alpha \simeq 0.006\,85$. For the frequency mismatch of fast alpha particles in thermal deuterons being negative, it requires the Lorentz factor of the alpha particles larger than 1.006 35; that is, the energy of the alpha particles has to be larger than 23.7 MeV. Since the fast alpha particles produced by the fusion reactions of thermal deuterons and tritons have the energy of only 3.5 MeV, they cannot drive the coupled relativistic electromagnetic ion cyclotron instabilities. Both the fast protons and the fast alphas in thermal deuterons cannot satisfy Eq. (53) to excite the decoupled quadratic instability as in contrast to the electrostatic case [23,27–29] especially at high harmonics.

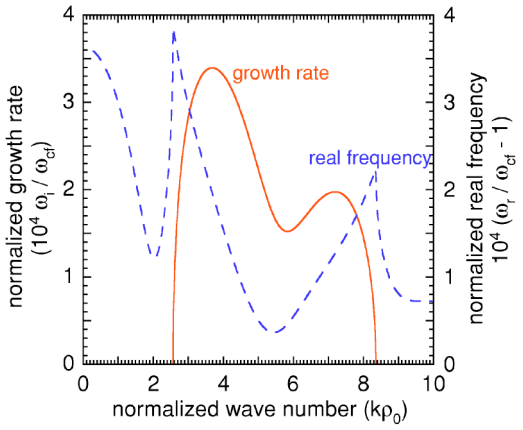

FIG. 1. (Color online) The normalized growth rate ω_i/ω_{cf} (the solid line) and the residue of the normalized real frequency $\omega_r/\omega_{cf}-1$ (the dash line) vs the normalized wave number $k\rho_0$ for the typical plasma parameters case of the electromagnetic ion cyclotron wave resonating with the first proton harmonic and the second deuteron harmonic.

A. Typical plasma parameters

We will consider fast 3.02-MeV protons, that are isotropically distributed in momentum space, in a thermal plasma of deuterons and neutralizing electrons. The external magnetic field is $B_0=3$ T. The thermal deuteron density is $n_d = 5\times 10^{13}$ cm^{-3}. The deuteron temperature is $T=10$ keV. The fast proton density is $n_p = 5\times 10^9$ cm^{-3}; that is, the density ratio of the fast protons and the thermal deuterons is $n_p/n_d = 0.0001$. Thus the corresponding plasma parameters are the deuteron plasma frequency $\omega_{pd}=6.58\times 10^9$ rad/s, the deuteron cyclotron frequency $\omega_{cd}=1.437\,54\times 10^8$ rad/s, the fast proton plasma frequency $\omega_{pp}=9.29\times 10^7$ rad/s, the relativistic fast proton cyclotron frequency $\omega_{cp} = 2.864\,43\times 10^8$ rad/s, the electron plasma frequency $\omega_{pe} = 3.99\times 10^{11}$ rad/s, the electron cyclotron frequency $\omega_{ce} = 5.28\times 10^{11}$ rad/s, the maximum gyroradius of the fast protons $\rho_0=8.4$ cm, and the gyroradius of a deuteron with the perpendicular thermal velocity $\rho_s=0.482$ cm. Also, $a_m = 0.154$ and $a_s=1.34$ (1.07) for $\ell=1$ (2). Since the deuteron cyclotron frequency is about half of the proton cyclotron frequency, the resonant cyclotron harmonic number of the deuterons is twice that of the fast protons.

Figure 1 shows the spectrums of the growth rate and the real frequency of the electromagnetic ion cyclotron wave,

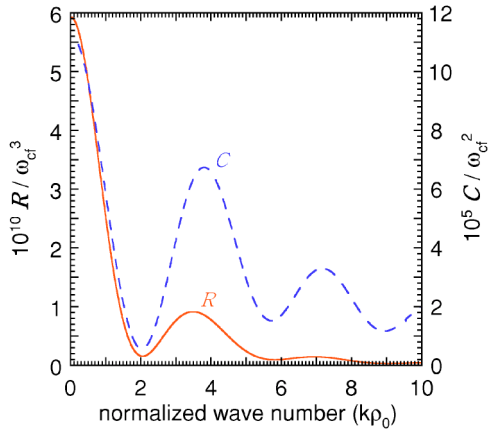

FIG. 2. (Color online) The normalized parameter R/ω_{cf}^3 (the solid line) and coefficient C/ω_{cf}^2 (the dash line) vs the normalized wave number $k\rho_0$.

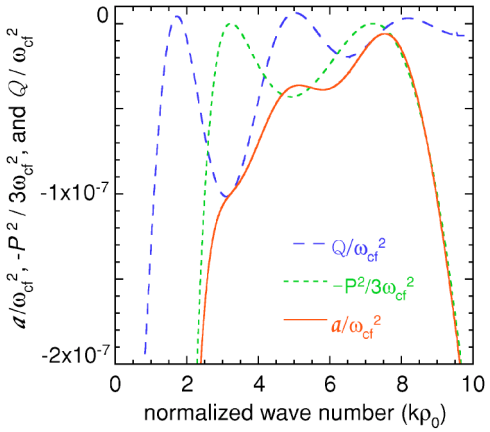

FIG. 4. (Color online) The normalized parameters a/ω_{cf}^2, $-P^2/3\omega_{cf}^2$, and Q/ω_{cf}^2 vs the normalized wave number $k\rho_0$.

that is resonant with first proton harmonic and second deuteron harmonic. Both are normalized by the fast proton cyclotron frequency, while the normalized real frequency is also deducted by the harmonic number (and will be henceforth called as the residue of the normalized real frequency). There are two peaks in this growth rate spectrum. Both peaks occurs near the peaks of the driving parameter R and the zeros of the parameter P as shown on Figs. 2 and 3, respectively; these are the characteristics of the maximum growth rate of the cubic instability as indicated in the analysis of previous section. The locations of corresponding R peaks are a little lower than those of the instability driving term C contributed by the fast ion second-order resonance because the absolute value of the nonresonant plasma dielectric A is smaller at higher wave phase velocity (i.e., lower k) as indicated in Eq. (21). The first (second) growth rate peak is at $k\rho_0=3.68$ (7.19), that is a little higher than the corresponding driving parameter R peak at $k\rho_0=3.48$ (6.93). This shifting is due to the weakening of the instability by a negative coefficient a as indicated in Eq. (37) while the absolute value of the coefficient a increases with lower $k\rho_0$ at the unstable regimes as indicated in Fig. 4, where the variation of the parameters Q and P are determined by the resonant harmonics of the fast and slow ions, respectively. The normalized peak growth rate at $k\rho_0=3.68$ (7.19) as shown on Fig. 1 is 3.40×10^{-4} (1.98×10^{-4}), that is in excellent agreement with 3.34×10^{-4} (1.98×10^{-4}) as predicted by the analytical result in Eq. (37). Equation (29) predicts that the peak growth rate occurs at $k\rho_0=2.67$, while the numerical result is $k\rho_0=3.68$. The residue of the normalized real frequency is 1.97×10^{-4} (1.27×10^{-4}) so that the ratio of the peak growth rate and the residue of the real frequency is 1.73 (1.56) that is also in excellent (good) agreement with the theoretical prediction of $\sqrt{3}$ for the cubic instability. Thus we conclude that the unstable growth rate spectrum is caused by the cubic relativistic electromagnetic ion cyclotron instability.

B. Slow ion temperature

If the temperature of the thermal deuterons is increased, the absolute value of the resonant slow ion dielectric coefficient D is also increased as shown on Fig. 5, while the co-

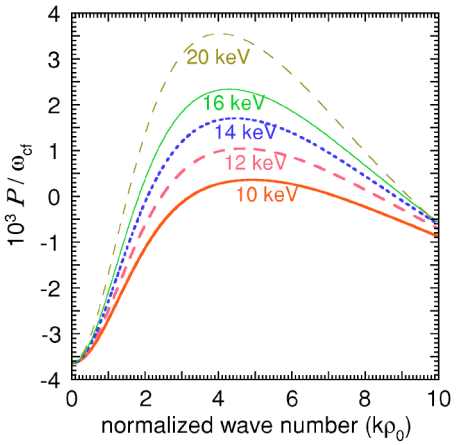

FIG. 3. (Color online) The normalized parameter P/ω_{cf} of the thermal deuterium temperature being 10, 12, 14, 16, and 20 keV vs the normalized wave number $k\rho_0$.

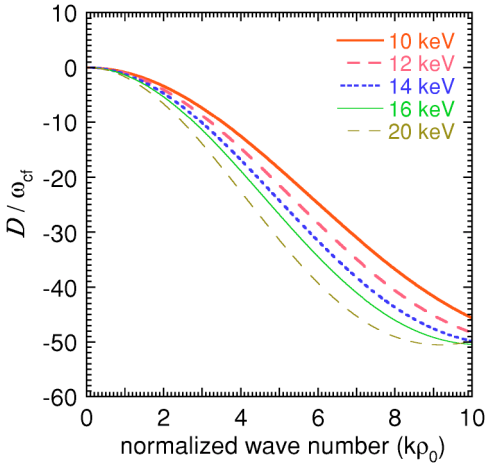

FIG. 5. (Color online) The normalized coefficient D/ω_{cf} of the thermal deuterium temperature being 10, 12, 14, 16, and 20 keV vs the normalized wave number $k\rho_0$.

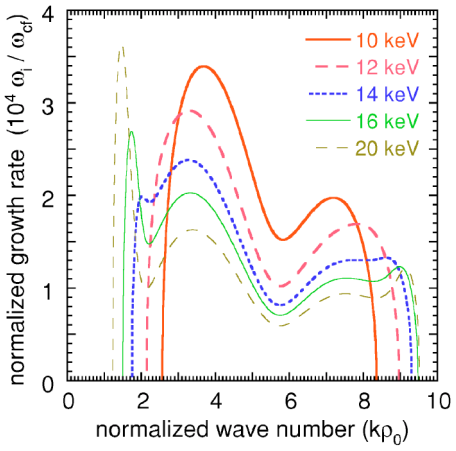

FIG. 6. (Color online) The normalized growth rate ω_i/ω_{cf} of the thermal deuterium temperature being 10, 12, 14, 16, and 20 keV vs the normalized wave number $k\rho_0$.

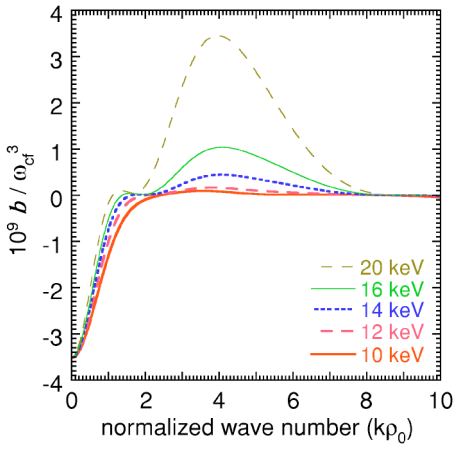

FIG. 8. (Color online) The normalized parameter b/ω_{cf}^3 of the thermal deuterium temperature being 10, 12, 14, 16, and 20 keV vs the normalized wave number $k\rho_0$.

efficients A, B, and C remain the same. From Eq. (18), we know that the parameter P is increased as also indicated on Fig. 3 and thus the wave number of first (second) $P=0$ corresponding to the first (second) growth rate peak moves toward a smaller (larger) value. This moving of the $P=0$ points shifts the first (second) growth rate peak as shown on Fig. 6, that also indicates the decreasing of the growth rate peaks. Two factors are responsible for this decreasing. The first is the corresponding driving parameter R becomes smaller as shown in Fig. 2 because the cubic root of R with a correction term $a/(3b^{2/3})$ decides the growth rate of the cubic instability as shown in Eq. (37). The other factor is the negative correction term. The higher the slow ion temperature and the parameter P, the higher the absolute value of the parameter a as shown in Fig. 7; while Fig. 8 shows that the parameter b only increases moderately because the first term (i.e., the driving parameter R) of b in Eq. (33) decreases and both the second and third terms increase. Therefore the correction term becomes large as shown in Fig. 9.

We shall consider the possibility of the coupled quadratic instability because the cubic correction term becomes large. The increase of the resonant slow ion dielectric coefficient D with the slow ion temperature also indicates the same possibility. The first term of condition (42) is proportional to the slow ion temperature so that this condition can be satisfied if the slow ion temperature is high enough. Figure 10 shows the relation of the peak growth rates and the slow ion temperature. At $T=10$ keV, the peak growth rate fits very well with the analytical prediction of the cubic instability while the prediction of the coupled quadratic instability is far too high. When the slow ion temperature is 15 keV and higher, the analytical prediction of the quadratic instability fits well with the peak growth rate calculated numerically. But, the cubic instability prediction is not. In other words, the same instability peak has transited from cubic to quadratic during the increasing of the slow ion temperature. It is also interesting to note that the wave numbers of the quadratic growth rate peaks remain almost constant as shown in Fig. 6. Equation (48) indicates that the peak growth rate is decreased with the increase of D, that is proportional to the $(s-1)/2$ power of the slow ion temperature. This explains that the peaks decrease with higher slow ion temperature as shown in Fig. 6.

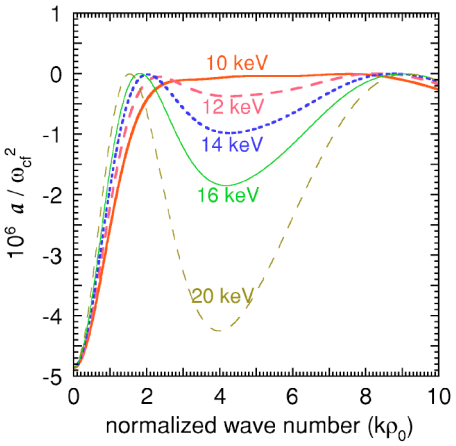

FIG. 7. (Color online) The normalized parameter a/ω_{cf}^2 of the thermal deuterium temperature being 10, 12, 14, 16, and 20 keV vs the normalized wave number $k\rho_0$.

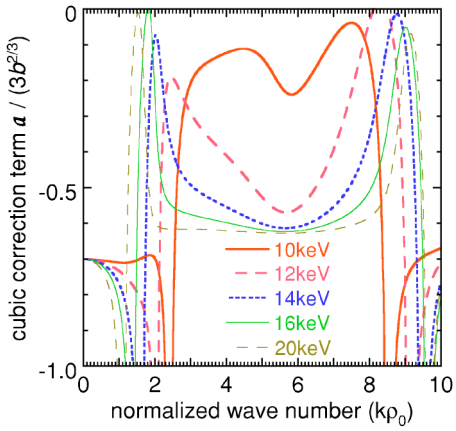

FIG. 9. (Color online) The cubic correction term $a/3b^{2/3}$ of the thermal deuterium temperature being 10, 12, 14, 16, and 20 keV vs the normalized wave number $k\rho_0$.

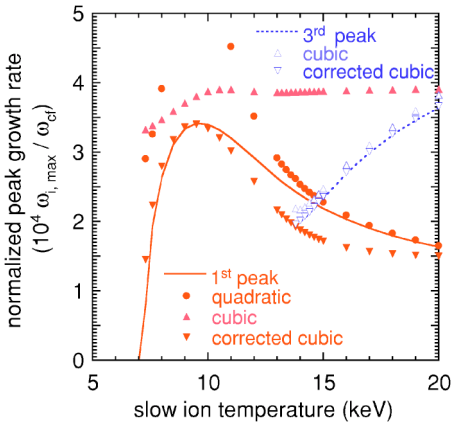

FIG. 10. (Color online) The normalized growth rate $\omega_{i,max}/\omega_{cf}$ of the first and third peaks vs the slow ion temperature. The wave numbers corresponding to the peaks are substituted into the analytical formulas Eqs. (48), (39), and (37) of the coupled quadratic instability, the cubic instability without and with correction term $a/3b^{2/3}$, respectively. Only the last two are shown for the third peak.

When the slow ion temperature is higher than 13.8 keV, a new instability branch appears and fits well with the cubic instability prediction, as shown in Fig. 10. This new instability branch corresponds to the third growth rate peaks at $k\rho_0 \leqslant 2$ of Fig. 6. As we discussed earlier, the wave number of the first $P=0$ moves from $k\rho_0 \simeq 3.24$ to that regime when the slow ion temperature is increased. Figure 4 shows that the parameter Q that is independent of the slow ion temperature is close to zero at $1.5 < k\rho_0 < 2$ regime. Since both conditions ($P \simeq 0$ and $Q \simeq 0$) are satisfied and the fitting is good, it is concluded that the cubic instability is responsible for this third peak and thus the new instability branch. The higher is the slow ion temperature; the lower is the wave number of the parameter $P=0$ and the growth rate peak, and the higher is the peak growth rate because the driving parameter R increases when the normalized wave number $k\rho_0$ is smaller than 2 as shown in Fig. 2.

Consider the effect of decreasing the slow ion temperature, instead of increasing it. For the $s=2$ case studied here, the cubic instability has a requirement on the plasma parameter for the instability to occur. The Alfvénic condition (31) can be rewritten in centimeter-gram-second system units as $(T/E_f) > 122B^2/n_s$. For the plasma parameters studied, the slow ion temperature of 10 keV is high enough to satisfy the Alfvénic condition. But, if the slow ion temperature is lower than 6.64 keV, this Alfvénic condition can be no longer satisfied. This threshold of the slow ion temperature is consistent with the numerical result shown in Fig. 10.

C. Slow ion density

We are going to study the effects of changing the slow ion density. The magnitude of the resonant dielectric of slow ions (i.e., the coefficient $|D|$) increases with the slow ion density. This shall have the similar effects caused by the slow ion temperature. In addition, the magnitude of the coefficient of the nonresonant plasma dielectric ($|A|$) will also increase.

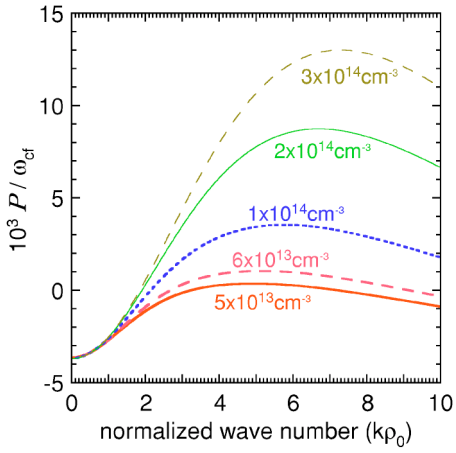

FIG. 11. (Color online) The normalized parameter P/ω_{cf} of the thermal ion density being 5×10^{13}, 6×10^{13}, 1×10^{14}, 2×10^{14}, and 3×10^{14} cm^{-3} vs the normalized wave number $k\rho_0$.

At the regime of small wave number, both the coefficients are linearly dependent on the slow ion density so that the parameter P remains almost unchanged. When the wave number is not small, the higher is the slow ion density, the higher is the parameter P as shown in Fig. 11. This moves the first $P=0$ to a lower wave number, but this movement is smaller as compared with the large magnitude increase of P and with that in the previous slow ion temperature case. The resultant growth rate spectrums are similar to those in the previous case and are shown in Fig. 12. When the slow ion density is increased, due to the coefficient D being more negative, the first growth rate peak decreases, and its corresponding wave number moves lower and then remains almost unchanged.

Figure 13 shows the peak growth rates obtained from the numerical simulation and analytical results for different slow ion densities. At $n_s=5\times10^{13}$ cm^{-3}, the growth rate of the first peak fits well with the prediction of the cubic instability. When the slow ion density has doubled, the first growth rate peak belongs to the coupled quadratic instability. Furthermore, a new instability branch begins to appear at n_s

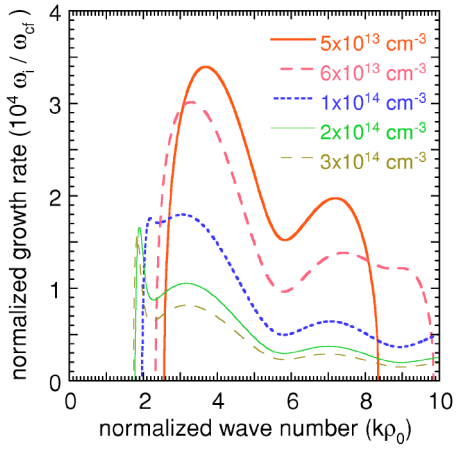

FIG. 12. (Color online) The normalized growth rate ω_i/ω_{cf} of the thermal ion density being 5×10^{13}, 6×10^{13}, 1×10^{14}, 2×10^{14}, and 3×10^{14} cm^{-3} vs the normalized wave number $k\rho_0$.

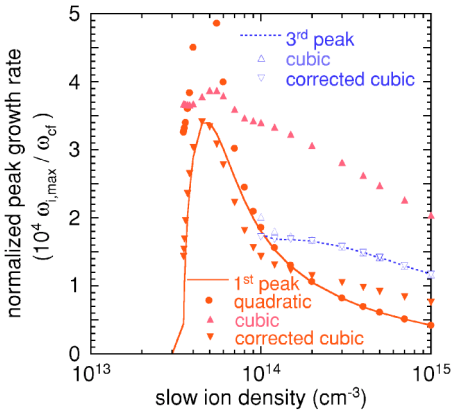

FIG. 13. (Color online) The normalized growth rate $\omega_{i,max}/\omega_{cf}$ of the first and third peaks vs the slow ion density. The wave numbers corresponding to the peaks are substituted into the analytical formulas Eqs. (48), (39), and (37) of the coupled quadratic instability, the cubic instability without and with correction term $a/3b^{2/3}$, respectively. Only the last two are shown for the third peak.

$=1\times10^{14}$ cm^{-3}, that corresponds to the third peak near $k\rho_0=2$ in Fig. 12. As in the slow ion temperature case, this third peak occurs where both the parameters P and Q are close to zero. However, there are two notable differences. The first is that the movement of this third peak toward a smaller wave number is much slower as shown in Fig. 12, because the movement of the wave number corresponding to $P=0$ toward a smaller value is also much slower, as discussed earlier. The other difference is that the amplitude of this third peak decreases with the increase of the slow ion density. As shown in Eq. (37), the peak growth rate of the cubic instability is proportional to the cubic root of the driving parameter R, where $R=C\Delta/A$. Because the absolute value of the nonresonant plasma dielectric A increases with the slow ion density, the driving parameter R decreases as shown in Fig. 14 so as the third peak growth rate. The Alfvénic condition (31) indicates that there is a threshold of the slow ion density for the cubic instability. The analytical threshold is $n_s=3.32\times10^{13}$ cm^{-3}, that is consistent with the numerical threshold shown in Fig. 13.

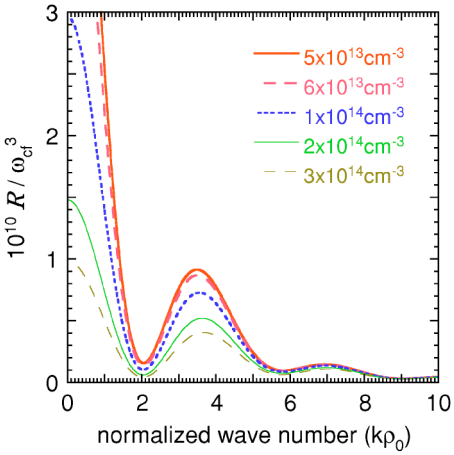

FIG. 14. (Color online) The normalized parameter R/ω_{cf}^3 of the thermal ion density being 5×10^{13}, 6×10^{13}, 1×10^{14}, 2×10^{14}, and 3×10^{14} cm^{-3} vs the normalized wave number $k\rho_0$.

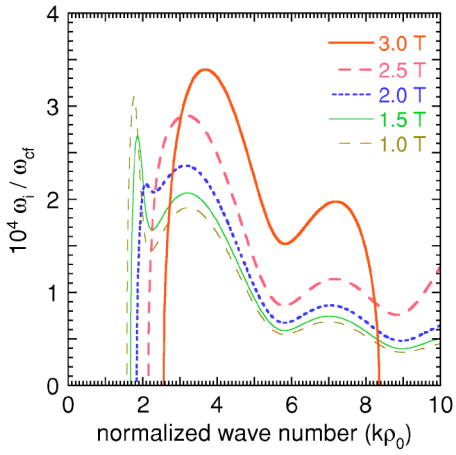

FIG. 15. (Color online) The normalized growth rate ω_i/ω_{cf} of the magnetic field being 3.0, 2.5, 2.0, 1.5, and 1.0 T vs the normalized wave number $k\rho_0$.

D. Magnetic field

The effects of varying magnetic field on the relativistic electromagnetic ion cyclotron instabilities are investigated. The reduction of the magnetic field decreases the ion cyclotron frequency and thus the wave frequency. The nonresonant plasma dielectric A is inversely proportional to the square of the magnetic field for the regime of low wave number and remains almost unchanged for high wave number. The normalized coefficients B/ω_{cf}, C/ω_{cf}^2, and D/ω_{cf} are all inversely proportional to the square of the magnetic field for a given $k^2\rho^2$; while the normalized frequency mismatch Δ/ω_{cf} remains constant. Both the increase of the coefficients A and D/ω_{cf} due to the lower magnetic field have similar effects as in the case of increasing the slow ion density. The normalized parameter P/ω_{cf} remains almost unchanged at the low wave number regime and increases at the high wave number regime; this moves the point of $P=0$ toward a lower wave number.

Figure 15 shows that the first growth rate peak also moves to a lower wave number with a smaller growth rate when the magnetic field is reduced. The decrease of the peak growth rate is due to the competition of two factors. The first is the increase of the normalized driving parameter R/ω_{cf}^3 for a weaker magnetic field as shown in Fig. 16. The other is that the correction term of Eq. (37) on the cubic instability becomes large and significantly reduces the peak growth rate, as shown in Fig. 17. Furthermore, when the cubic correction is large at low magnetic field, the predictions of the coupled quadratic instability agrees well with the numerical results. For the coupled quadratic instability, the first growth rate peak is located at a fixed wave number as shown in Fig. 15, which also shows that a third peak appears when the magnetic field is equal to or lower than 2 T. Due to the movement of $P=0$, this third growth rate peak moves to a smaller wave number toward where $Q\simeq0$. The third peak growth rate becomes higher because the normalized driving parameter R/ω_{cf}^3 increases for a lower wave number. This new instability branch agrees well with the prediction of the cubic instability with or without the correction term as indicated in

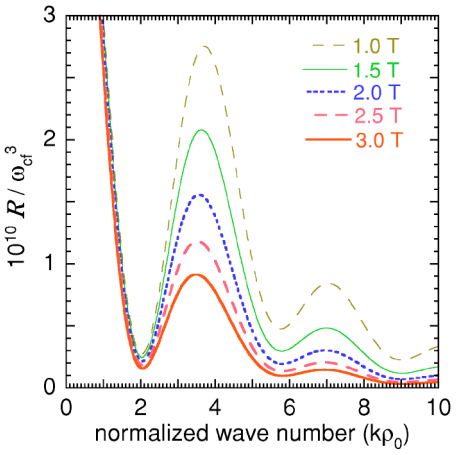

FIG. 16. (Color online) The normalized parameter R/ω_{cf}^3 of the magnetic field being 3.0, 2.5, 2.0, 1.5, and 1.0 T vs the normalized wave number $k\rho_0$.

Fig. 17. The numerical result shows that there is no instability as the magnetic field B is larger than 3.55 T, while the analytical prediction of the Alfvénic behavior is 3.68 T; the agreement is good.

E. Fast ion density

The scalings of the peak growth rates on the fast ion density are studied. For the cubic instability, the analytical peak growth rate is scaled as the cubic root of the fast ion density as indicated in Eq. (39); while it is the square root for the coupled quadratic instability as shown in Eq. (48). For both the cubic and the coupled quadratic instabilities to be shown on one set of data, we have changed the plasma parameters with a higher slow ion density of 2×10^{14} cm^{-3}. Figure 18 shows the growth rates of the first and third peaks obtained numerically and those analytically predicted by the cubic and the coupled quadratic instabilities for different fast ion densities. The first and the third growth rate peaks agree very well with the coupled quadratic and cubic predictions, respectively. The normalized peak growth rate is scaled as the 0.485 (0.476) and 0.347 (0.348) power of the fast ion density for the coupled quadratic instability and the cubic instability from the numerical calculation (analytical prediction), respectively.

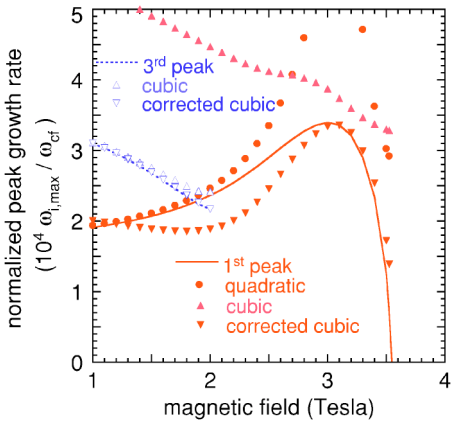

FIG. 17. (Color online) The normalized growth rate $\omega_{i,max}/\omega_{cf}$ of the first and third peaks vs the magnetic field. For the analytical predictions of the coupled quadratic instability, the cubic instability without and with correction term $a/3b^{2/3}$, the wave numbers corresponding to the peaks are substituted into Eqs. (48), (39), and (37), respectively. Only the last two are shown for the third peak.

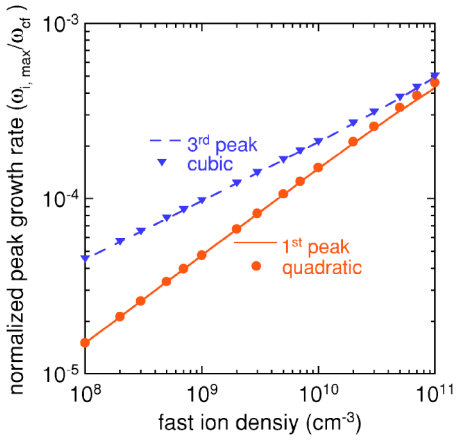

FIG. 18. (Color online) The normalized growth rate $\omega_{i,max}/\omega_{cf}$ of the first and third peaks vs the fast ion density for the plasma parameters with a higher slow ion density of 2×10^{14} cm^{-3}. For the analytical predictions of the coupled quadratic instability and the cubic instability, the wave numbers corresponding to the peaks are substituted into Eqs. (48) and (39), respectively.

V. DISCUSSION AND SUMMARY

The relativistic electromagnetic ion cyclotron instabilities are reactive. The peak growth rate is proportional to the cubic or square root of fast ion density, depending on the instability coupling mechanisms. Because fast ion density in typical plasmas is small, these scalings make the relativistic instabilities more important than the resistive electromagnetic ion cyclotron instability driven by classical inversed Landau damping [39,40]. The growth rates for typical plasma parameters are much larger than those of the classical resistive instability [39,40]. Thus the contribution from the inversed Landau damping, that depends on specific momentum profile, is neglected in our studies for focusing on the interesting characteristics of the instabilities. Nevertheless, it is straightforward to include this effect when it is necessary and the momentum profile is given.

Both the cubic and coupled quadratic instabilities require a negative frequency mismatch, while the decoupled quadratic instability does not have this requirement. Consider a fast ion with its harmonic cyclotron frequency lower than the wave frequency. When the fast ion loses energy to the wave, its harmonic cyclotron frequency will increase. The reverse is true for a slow ion. In both cases, their harmonic cyclotron frequencies are closer to the wave frequency. Therefore the resonance interactions are enhanced. Consider the collective effects. The second-order resonance of the fast ion contributes a positive dielectric for both sides of the wave frequency being higher or lower than the harmonic fast ion cyclotron

frequency. As also indicated in Eq. (11), the first-order resonance of slow ion gives a positive (negative) dielectric for the wave frequency being lower (higher) than the harmonic slow ion cyclotron frequency. A pair of complex conjugate roots is possible only when both resonant dielectrics are positive. Thus the instabilities require that the harmonic slow ion cyclotron frequency is larger than that of the fast ion and the wave frequency is in between.

The cubic and quadratic powers of the peak growth rates of the cubic and coupled quadratic instabilities, respectively, depend on the coefficient C of the fast ion driving second-order resonance and the frequency mismatch. The higher the driving, the higher the peak growth rate as expected. The higher frequency mismatch indicates larger room for the difference between the wave frequency and the harmonic fast ion cyclotron frequency, because the wave frequency is between the harmonic cyclotron frequencies of fast and slow ions. On the other hand, the cubic and quadratic powers of the peak growth rates are inversely proportional to the inertias, that is, the nonresonant plasma dielectric A and the resonant slow ions dielectric coefficient D, respectively. The quadratic power of the peak growth rate of the decoupled quadratic instability is proportional to the driving, is inversely proportional to the nonresonant plasma dielectric, but does not depend on the frequency mismatch.

The instabilities studied here have interesting characteristics because the nonresonant plasma dielectric (i.e., the plasma inertia) is usually a large negative number due to the wave magnetic field effect and the instability driving term is proportional to the square of the derivative of the Bessel function instead of the Bessel function for the relativistic electrostatic ion cyclotron instabilities. The latter shifts the wave number location of the growth rate peak while the former has profound effects. It ruins the decoupled quadratic instability because a positive nonresonant plasma dielectric is needed for this instability. For the cubic and quadratic instabilities due to the coupling of the fast and slow ion cyclotron harmonics, the wave magnetic field causes the unstable conditions to require the resonant slow ion cyclotron harmonic number being 1 or 2. Thus high harmonics are stable. For the coupled quadratic instability, the wave magnetic field can slightly increase the growth rate because it can reduce the dielectric of the resonant harmonic slow ion cyclotron. But, for the cubic instability, the wave magnetic field decreases the peak growth rate because it is inversely proportional to the cubic root of the nonresonant plasma dielectric A (i.e., the plasma inertia). The contribution of the wave magnetic field also imposes a threshold (ceiling) on the slow ion temperature and density (the external magnetic field and the fast ion energy) for the cubic instability. The Alfvén velocity is required to be low. This Alfvénic behavior is important for application in experiments. The Alfvénic behavior and the difference between fast protons and alphas in thermal deuterons (e.g., the first proton harmonic is most unstable and the first alpha harmonic is stable) are consistent with the experimental measurements of ion cyclotron emissions [34–38]. For a complete explanation of the ion cyclotron emissions observed in experiments, the coupling of the electromagnetic and electrostatic modes for relativistic ion cyclotron instabilities is being studied.

The instability transition never discovered before is interesting and may be important for application. As we understand from previous cyclotron instability studies [1,3] with [23,28] and without [41] relativistic effect, cubic and quadratic instabilities usually have different growth rate spectra at different wave vectors, different harmonics, and/or distinct plasma parameters. Even when their peaks are close to each other, they are separated. One may dominate for a set of plasma parameters. When the plasma parameters are changed, the growth rate of the dominated one may decrease while the other may increase and even become dominant. After all, they are two separated peaks and there is a valley in the growth rate spectrum between them. Also, the resultant particle dynamics and the nonlinear saturation mechanisms are very different for the cubic and quadratic instabilities. However, the relativistic electromagnetic ion cyclotron instabilities studied here for fast protons in thermal deuterons have the cubic and quadratic instabilities, representing different resonance coupling mechanisms, at the same growth rate peak for different plasma parameters. By moderately changing plasma parameters, the same growth rate peak transits from the cubic instability to the quadratic instability. The transition parameters are related to the threshold (or ceiling) condition of the Alfvénic behavior. Furthermore, while the transition occurs, a different cubic instability branch appears and coexists with the quadratic branch. This cubic branch is different than the original cubic branch. The instability transition may be important for applications, since the nonlinear saturation, the resultant particle dynamics, and the instability characteristics (e.g., absolute or convective) depend on the resonance coupling mechanism and the scaling and detail of the growth rate spectrum.

There are a few issues not studied here. The nonlinear saturation mechanisms determine the saturation level of the wave growth and the resultant fast ion dynamics and profiles. The absolute or convective growth of the instabilities is important when plasmas are not uniform. Plasma devices usually have a nonuniform confining magnetic field. The drift motion of the fast ions associated with the nonuniform magnetic field would move the fast ions in and out of the interaction regimes. The discussions [28] on these issues for the relativistic electrostatic ion cyclotron instabilities may be applicable to the instabilities studied here; however, these are not within the scope of this paper.

In summary, the physics of relativistic electromagnetic ion cyclotron instabilities have been studied. The cubic and quadratic instabilities from the coupling of second-order fast and first-order slow ion cyclotron resonances require a negative harmonic cyclotron frequency mismatch, as demanded by resonance enhancement and positive resonant dielectrics in the dispersion relation. Their peak growth rates are proportional to the cubic and square roots, respectively, of the fast ion density and Lorentz factor -1. These scalings make the relativistic effect more important than the inversed Landau damping mechanism for driving electromagnetic ion cyclotron instability. The wave magnetic field is important to determine the instabilities' characteristics and unstable conditions, which are quite different with the relativistic electrostatic ion cyclotron instabilities. The peak growth rates and their locations as well as the threshold (ceiling) of the slow

ion density and temperature (the external magnetic field) are obtained analytically and compared in good agreement with those from numerical calculations. This Alfvénic behavior found here is mainly due to the wave magnetic field and is important for application in experiments. When the slow ion density or temperature (the external magnetic field or the fast ion energy) is about two times (half) the threshold (ceiling), the same growth rate peak transits from the cubic instability to the coupled quadratic instability and a different cubic instability branch appears. This instability transition is interesting and remains to be verified by experiments. The coupling of the relativistic electromagnetic and electrostatic ion cyclotron instabilities deserves further studies. While the physics studied are emphasized, in additional to in the laboratory, the relativistic electromagnetic ion cyclotron instabilities may occur in nature and particularly in some astrophysical radiation sources.

ACKNOWLEDGMENT

This work was supported by the National Science Council of the Republic of China, Taiwan.

[1] K. R. Chu, Rev. Mod. Phys. **76**, 489 (2004).
[2] K. R. Chen, J. M. Dawson, A. T. Lin, and T. Katsouleas, Phys. Fluids B **3**, 1270 (1991).
[3] T. H. Stix, *Waves in Plasmas* (AIP, Woodbury, NY, 1992).
[4] D. E. Baldwin, I. B. Bernstein, and M. P. H. Weenik, Adv. Plasma Phys. **3**, 18 (1969).
[5] K. R. Chen and K. R. Chu, IEEE Trans. Microwave Theory Tech. **34**, 72 (1986).
[6] K. R. Chu, in *Wave Heating and Current Drive in Plasmas*, edited by V. L. Granatstein and P. L. Colestock (Gordon and Breach, New York, 1985), Chap. 7.
[7] *Application of High Power Microwaves*, edited by A. V. Gaponov-Grekhov and V. L. Granatstein (Artech House, Boston, MA, 1994).
[8] N. J. Fisch, Rev. Mod. Phys. **59**, 175 (1987).
[9] N. J. Fisch and J. M. Rax, Nucl. Fusion **32**, 549 (1992).
[10] N. J. Fisch, Plasma Phys. Controlled Fusion **35**, A91 (1993).
[11] I. H. Hutchinson, *Principles of Plasma Diagnostics*, 2nd ed. (Cambridge University Press, New York, 2002).
[12] F. F. Chen, *Introduction to Plasma Physics and Controlled Fusion*, 2nd ed. (Plenum, New York, 1983), Vol. 1.
[13] N. A. Krall and A. W. Trivelpiece, *Principles of Plasma Physics* (San Francisco Press, San Francisco, 1986), pp. 409, 450.
[14] R. Geller, *Electron Cyclotron Resonance Ion Source and ECR Plasmas* (Institute of Physics, London, 1996), p. 236.
[15] C. S. Wu and L. C. Lee, Astrophys. J. **230**, 621 (1979).
[16] D. B. Melrose, *Instabilities in Space and Laboratory Plasmas* (Cambridge University Press, London, 1986).
[17] T. Tajima and K. Shibata, *Plasma Astrophysics* (Addison-Wesley, Reading, MA, 1997).
[18] R. Q. Twiss, Aust. J. Phys. **11**, 564 (1958).
[19] J. Schneider, Phys. Rev. Lett. **2**, 504 (1959).
[20] A. V. Gaponov-Grekhov, Izv. Vyssh. Uchebn. Zaved., Radiofiz. **2**, 450 (1959); **2**, 836 (1959).
[21] V. V. Zheleznyakov, Izv. Vyssh. Uchebn. Zaved., Radiofiz. **3**, 57 (1960).
[22] R. A. Blanken, T. H. Stix, and A. F. Kuckes, Phys. Fluids **11**, 945 (1969).
[23] K. R. Chen, Phys. Lett. A **181**, 308 (1993).
[24] K. R. Chen, W. Horton, and J. W. van Dam, Phys. Plasmas **1**, 1195 (1994).
[25] K. R. Chen, Phys. Rev. Lett. **72**, 3534 (1994).
[26] K. R. Chen, Nucl. Fusion **35**, 1769 (1995).
[27] K. R. Chen, Phys. Lett. A **247**, 319 (1998).
[28] K. R. Chen, Phys. Plasmas **7**, 844 (2000); **7**, 857 (2000).
[29] K. R. Chen, Phys. Plasmas **10**, 1315 (2003).
[30] K. R. Chen, Phys. Lett. A **326**, 417 (2004).
[31] H. P. Furth, R. J. Goldston, S. J. Zweben, and D. J. Sigmar, Nucl. Fusion **30**, 1799 (1990).
[32] N. J. Fisch and J. M. Rax, Phys. Rev. Lett. **69**, 612 (1992).
[33] R. J. Hawryluk, Rev. Mod. Phys. **70**, 537 (1998).
[34] G. A. Cottrell and R. O. Dendy, Phys. Rev. Lett. **60**, 33 (1988).
[35] J. Team, Nucl. Fusion **32**, 187 (1992).
[36] G. A. Cottrell, V. P. Bhatnagar, and O. da Costa, Nucl. Fusion **33**, 1365 (1993).
[37] S. Cauffman, R. Majeski, K. G. McClements, and R. O. Dendy, Nucl. Fusion **35**, 1597 (1995).
[38] K. G. McClements, C. Hunt, R. O. Dendy, and G. A. Cottrell, Phys. Rev. Lett. **82**, 2099 (1999).
[39] B. Coppi, Phys. Lett. A **172**, 439 (1993).
[40] N. N. Gorelenkov and C. Z. Cheng, Phys. Plasmas **2**, 1961 (1995).
[41] R. O. Dendy, C. N. Lashmore-Davies, and K. F. Kam, Phys. Fluids B **4**, 3996 (1992).
[42] K. G. McClements *et al.*, Phys. Plasmas **3**, 543 (1996).
[43] G. A. Korn and T. M. Korn, *Mathematical Handbook for Scientists and Engineers* (Dover, New York, 1968), p. 23.